PCCP

Cite this: *Phys. Chem. Chem. Phys.*, 2012, **14**, 5849–5854

www.rsc.org/pccp

PAPER

Computational study of the adsorption and dissociation of phenol on Pt and Rh surfaces†

Maija L. Honkela,*[ab] Jonas Björk[bc] and Mats Persson[bd]

Received 20th December 2011, Accepted 28th February 2012
DOI: 10.1039/c2cp24064e

The adsorption of phenol on flat and stepped Pt and Rh surfaces and the dissociation of hydrogen from the hydroxyl group of phenol on Pt(111) and Rh(111) were studied by density functional calculations. On both Pt(111) and Rh(111), phenol adsorbs with the aromatic ring parallel to the surface and the hydroxyl group tilted away from the surface. Furthermore, adsorption on stepped surfaces was concluded to be unfavourable compared to the (111) surfaces due to the repulsion of the hydroxyl group from the step edges. Transition state calculations revealed that the reaction barriers, associated with the dissociation of phenol into phenoxy, are almost identical on Pt and Rh. Furthermore, the oxygen in the dissociated phenol is strongly attracted by Rh(111), while it is repelled by Pt(111).

1 Introduction

Due to environmental concerns and depletion of oil reserves, the interest towards biomass as a source for fuels has increased rapidly during the last decade. The main disadvantage of liquids derived from biomass, through processes such as pyrolysis, is that they include as much as 50 wt% oxygen.[1,2] High oxygen content causes several undesired properties, such as low volatility, corrosiveness, thermal instability and tendency to polymerize under exposure to air.[1,3] Thus oxygen needs to be removed, at least partially, to increase the energy value and stability of the fuel.

Oxygen-removal can be carried out with a hydrodeoxygenation (HDO) process in the presence of hydrogen on a catalyst that is conventionally a sulfided CoMo or NiMo catalyst on γ-Al_2O_3.[2] The sulfidation process of these catalysts contaminates the fuel by sulfur species. Loss of sulfur from the catalyst surface decreases its activity unless extra sulfur is added to the feed.[2] This results in increased contamination of the product. Another challenge is the γ-Al_2O_3 support that has been found to be unstable under HDO conditions and that catalyzes coke formation because of its acidity.

Due to disadvantages of sulfur-catalysts, research into sulfur-free catalysts has increased. It is expected that non-sulfided catalysts work at lower temperatures, which reduces the coke formation and thus decreases the deactivation of the catalyst. Furthermore, the problems with the γ-Al_2O_3 support can be avoided if a different support material is used. One promising alternative for non-sulfided catalysts has been to use transition metal catalysts, such as Pt, Rh or Pd, on the ZrO_2 support.[4]

As biomass-based liquids are complex mixtures of hydrocarbons, their reactions are often studied using model components.[2,4] Typical model components for wood-based liquids are phenol, anisole (methoxybenzene) and guaiacol (2-methoxyphenol), the chemical structures of which are illustrated in Fig. 1.

Although several computational studies discuss the behavior of benzene on Pt, Rh and Pd surfaces (reviewed by Jenkins[5]), only a few discuss the behavior of aromatic oxygen-containing components on these surfaces.[5–8] For example, Bonalumi and co-workers[7] studied the adsorption of anisole and its derivatives on the Pt(111) surface using density functional theory (DFT) cluster calculations. They concluded that the studied molecules are less strongly bonded to the surface compared to the parent molecule benzene. In the case of anisole, this effect is thought to be a result of steric hindrance of the methoxy group.[8] Furthermore, Orita and Itoh studied phenol on Pd(111), illustrating that also this molecule adsorbs weaker compared to benzene.[6]

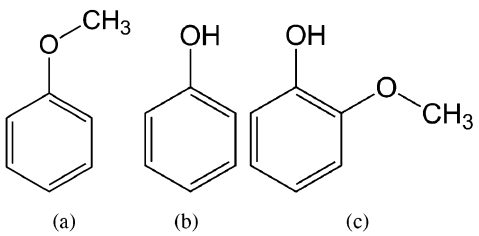

Fig. 1 Structures of (a) anisole, (b) phenol and (c) guaiacol.

[a] *Department of Biotechnology and Chemical Technology, Aalto University, P.O.Box 16100, FI-00076 Aalto, Finland. E-mail: maija.honkela@gmail.com*
[b] *The Surface Science Research Centre, The University of Liverpool, Liverpool L69 3BX, UK*
[c] *Department of Physics, Chemistry and Biology, IFM, Linköping University, 581 83 Linköping, Sweden*
[d] *Department of Applied Physics, Chalmers University of Technology, SE 412 96 Göteborg, Sweden*
† Electronic supplementary information (ESI) available. See DOI: 10.1039/c2cp24064e

Due to its chemical stability, phenol is thought to be one of the components most resistant to oxygen removal.[2,9] Furthermore, phenol is a typical intermediate in the deoxygenation reactions of more complicated aromatic oxygen-containing molecules. Because of this, a detailed theoretical understanding of its adsorption on different catalytic surfaces is of paramount interest. Although a few theoretical studies considering different oxygen-containing model components on Pt, Pd and Rh exist, as presented above, no studies consider the adsorption of phenol on Pt and Rh. Experimental studies, on the other hand, have addressed adsorption geometry and dissociative adsorption of phenol as phenoxy (hydrogen dissociated from the hydroxyl group) on Pt(111)[10] and Rh(111)[11] surfaces.

The Pt(111) and Rh(111) surfaces are the most stable facets of the Pt and Rh crystals, and probably form during catalyst preparation. Still, catalytic reactions often occur preferably on surface steps and edges.[12]

In this study, we use phenol as an oxygen-containing model component for biomass-based liquids. We will discuss the behavior of phenol on Pt(111), Rh(111) and stepped Pt and Rh surfaces based on periodic DFT calculations. The aim of the study is to elucidate the adsorption configurations as well as to assess the relative adsorption strengths on the different substrates. Furthermore, because experimental studies have shown phenol to adsorb as phenoxy under certain conditions,[10,11] adsorption of phenoxy on Pt(111) and Rh(111) will also be addressed. In particular, the catalytic effect of the two surfaces on the dissociation of phenol into phenoxy will be unraveled from transition state calculations. The aim of the study is to understand the adsorption and reactivity of phenol on clean Pt and Rh surfaces, but it should be noted that HDO reaction conditions could correspond to hydrogen covered surfaces.

The paper is structured in the following way: first, we give a brief summary of the available experimental results in Section 2 followed by an outline of the theoretical methods in Section 3. The results and discussion part of the article first discusses the adsorption of phenol (Section 4.1) on Pt(111) and Rh(111), followed by the stepped Pt(211) and Rh(211) surfaces. We finalize the results by discussing the dissociation of phenol into phenoxy on Pt(111) and Rh(111) in Section 4.2.

2 Experimental information

Experimental studies of the adsorption of phenol on both Pt(111)[10] and Rh(111)[11] exist. For example, Ihm and White[10] studied the adsorption and dissociation of deuterium-labeled forms of phenol on Pt(111) with temperature-programmed desorption (TPD), high-resolution electron energy loss spectroscopy (HREELS) and X-ray photoelectron spectroscopy (XPS). They observed that at 125 K phenol adsorbs intact on the surface. Upon heating to 200 K phenol completely dissociates by O–H breakage and the formed phenoxy structure adsorbs through η^5–π-adsorbed-quinoidal geometry.

Xu and Friend[11] studied phenol on Rh with temperature-programmed reaction and XPS. At 100 K both molecular phenol as well as phenoxy species were observed. At 300 K only the chemisorbed phenoxy intermediate was obtained. In experiments with surface deuterium on Rh(111) no reversible C–H bond activation was observed indicating that the phenyl ring is not oriented parallel to the surface.

3 Computational details

The calculations were performed within the framework of periodic density functional theory (DFT) using the VASP code[13] interfaced to the Atomic Simulation Environment[14] (ASE). Ion–core electron interactions were described using the projected augmented wave method[15,16] and the PW91 functional[17] was used to describe exchange and correlation effects.

The flat Pt(111) and Rh(111) surfaces were modeled by four layered slabs separated by at least 20 Å of vacuum, and $p(5 \times 5)$ surface unit cells. The Pt(211) and Rh(211) stepped surfaces, which in a step notation are given by [3(111) × (100)], consist of three atoms wide terraces of (111) structure, separated by one atom high steps of (100) structure. The stepped surfaces were modeled by four-layer slabs, and surface unit cells of four atoms in the direction running along the terraces and two terraces wide (4 × 6 atoms per surface unit cell and slab layer). Computed bulk lattice constants were used, 3.986 Å and 3.844 Å for Pt and Rh, respectively.

In all calculations a 2×2 k-point sampling together with the Methfessel–Paxton smearing scheme[18] of first order with a smearing width of 0.2 eV were used. A kinetic energy cutoff of 400 eV and a convergence criterion for total energies of 10^{-6} eV were used. All results presented in this paper were obtained from spin-restricted calculations. For the adsorption of phenoxy radicals, spin-polarized calculations were carried out, illustrating that the spin-polarization of phenoxy is quenched once adsorbed on either Pt or Rh (see ESI†).

Structural optimizations were performed until the forces acting on the atoms in adsorbed molecules and the two outermost slab layers were smaller than 0.02 eV Å^{-1}. Binding energies on the various surfaces were defined as

$$E_{\mathrm{bind}} = -[E_{\mathrm{phenol@Pt/Rh}} - (E_{\mathrm{phenol}} + E_{\mathrm{Pt/Rh}})] \qquad (1)$$

where $E_{\mathrm{phenol@Pt/Rh}}$ is the total energy of phenol on a Pt or Rh surface, E_{phenol} is the total energy of phenol under vacuum, and $E_{\mathrm{Pt/Rh}}$ is the total energy of the corresponding free Pt or Rh surface. In this convention, the larger the positive value of E_{bind} the stronger is the adsorption.

Transition state calculations were carried out following the approach described in ref. 19 using a combination of the *climbing image nudged elastic band*[20,21] (CI-NEB) and *dimer*[22,23] methods. In short, CI-NEB was used to find an initial estimate of the transition state. This estimate was then used to set up the starting configuration (central image and dimer) in the *dimer* method. The structural optimization of the dimer was performed until the forces acting on the atoms on the central image were smaller than 0.02 eV Å^{-1}.

4 Results and discussion

4.1 Adsorption of molecular phenol

4.1.1 Flat surfaces. For phenol on Pt(111) and Rh(111) several parallel and vertical adsorption configurations were structurally optimized and compared. On both surfaces, similar adsorption configurations were found to be the most stable ones

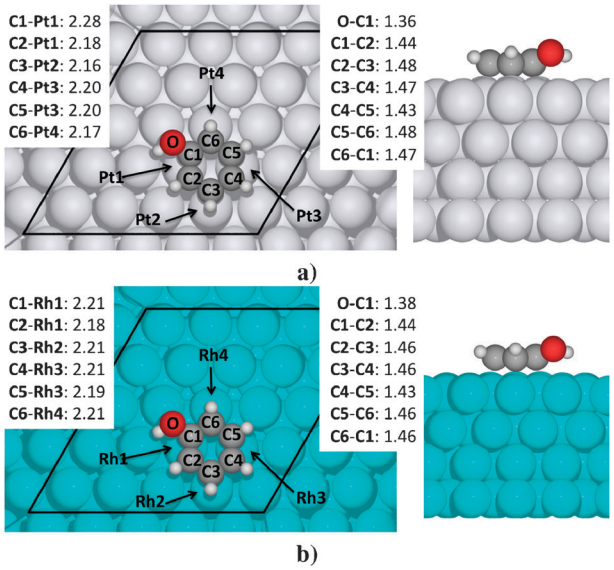

Fig. 2 Top and side views of the most stable configurations of phenol on (a) Pt(111) and (b) Rh(111). The black lines in the top views indicate the unit cells used in the calculations. The tabulated bond lengths are in units of Å. Additional adsorption configurations can be found in the ESI.†

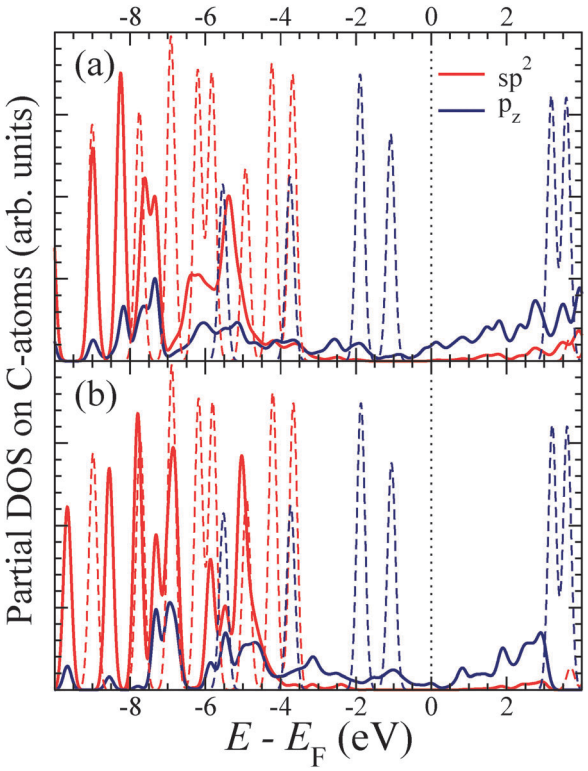

Fig. 3 PDOS of the C-atoms in phenol for the molecule adsorbed in its most stable adsorption configurations on (a) Pt(111) and (b) Rh(111), respectively. The thin dashed lines show the PDOS for phenol under vacuum, while the solid lines show the PDOS for phenol adsorbed on the two surfaces. The vacuum level of the molecule under vacuum and the molecule on a surface has been aligned in the two plots. The adsorption geometries are depicted in Fig. 2.

as illustrated in Fig. 2. In these configurations the molecule is adsorbed parallel to the surface with both the aromatic ring and the oxygen of the hydroxyl group above bridge sites. The molecule is oriented such that the main axis of its aromatic ring spans a 30° angle with the close-packed direction of the (111) surface. The adsorption is strongest on Rh(111), with a binding energy of 2.79 eV compared to 2.23 eV for Pt(111). Note that these energies are substantially larger than the calculated binding energy of 1.39 eV for phenol on Pd(111).[6] However, this trend of binding energies is consistent with the trend of calculated C atom binding energies on these surfaces. The C atom binding energy was shown to be a good descriptor for the binding energies of hydrocarbons on transition metal surfaces.[24]

Vertical configurations resulted in a substantially weaker adsorption of phenol on both surfaces (binding energies of 1.09 eV on Pt(111) and 1.15 eV on Rh(111)). Hence, phenol has a preferred adsorption configuration with the ring closely parallel to the Pt(111) as well as the Rh(111) surface, in agreement with experimental results for phenol on Pt(111).[10] The adsorption height of the center-of-mass of the molecule above the outermost surface layer was found to be 2.30 Å on Pt(111) and 2.29 Å on Rh(111).

Despite the parallel adsorption configuration of the aromatic ring on Pt(111) and Rh(111), there are distinct structural changes of phenol upon adsorption on both surfaces. This is best illustrated in the side views of the adsorption configurations in Fig. 2. For both Pt(111) and Rh(111) the C-atoms bond directly to the surface atoms, with their adjoining H-atoms pointing slightly away from the surface. Furthermore, the average C–C bond length is elongated from 1.40 Å (for phenol under vacuum) to 1.46 Å and 1.45 Å on Pt(111) and Rh(111), respectively. These are indications of the C-atoms slightly changing their character from sp^2 to sp^3 hybridization. Finally, the hydroxyl group was found to point away from the surfaces.

In order to understand the bonding mechanism in more detail, the partial density of states (PDOS) was calculated for the C-atoms in the aromatic ring of the most stable adsorption configurations of phenol on Pt(111) and Rh(111), as well as for phenol under vacuum, Fig. 3. Considering the molecule under vacuum, the PDOS is well described by contributions from orbitals of sp^2 and p_z. Notice that for the molecule under vacuum these orbitals do not overlap considerably. For the molecule adsorbed on the two surfaces sp^3 hybridization, mentioned above, becomes evident. This is seen as the sp^2 contributions are mixed with p_z orbitals, in particular at energies below E_F −4 eV. The bonding mechanism has a typical covalent character as the two p_z contributions aligned closest to the Fermi level are split into a bonding and an anti-bonding band. The more favorable adsorption on Rh compared to Pt may be attributed to the larger occupancy of the anti-bonding band for phenol adsorbed on Pt(111).

Notably, Tan and co-workers[8] observed that also with anisole the methoxy group turns away from the Pt(111) surface. The angle between oxygen and surface was found to be 12.4° while oxygen and methyl in the methoxy group had an angle of 2.0° and were thus again almost parallel to the surface. Now in our study with phenol on Pt(111) the angle between oxygen and surface was found to be 22.9° and thus clearly higher than the value with anisole. The same increase in C–C bond length was also observed for anisole[8] (1.38 Å for the free molecule and 1.44 Å on the surface) as for phenol in our study.

4.1.2 Stepped surfaces. Step edges on substrates are often considered as preferable sites for catalysis, which is why it is interesting to investigate the interaction of adsorbates with these sites. Here, the adsorption of phenol on the vicinal Pt(211) and Rh(211) surfaces was studied.

The most stable adsorption configurations on both the stepped surfaces are illustrated in Fig. 4. Reminiscent with the (111) surfaces, the molecule is adsorbed with the aromatic ring centered above a bridge site. The main axis of the molecule is rotated 90° with respect to the close-packed rows running along the steps, but with the hydroxyl group pointing in opposite directions on the two surfaces.

Interestingly, on neither Pt nor Rh the steps make phenol to adsorb stronger than on the terraces. Compared to the (111)-facets, the binding energy on Pt(211) is reduced by 0.64 eV, while on Rh(211) it is reduced by 1.00 eV, as shown in Table 1. The decrease in the adsorption strength can be assigned to the repulsion of the hydroxyl group from the steps. Furthermore, the larger decrease in the adsorption strength on Rh compared to Pt is explained by the size of the terraces, which are narrower for Rh(211) than for Pt(211) and force the hydroxyl group to turn away from the Rh(211) step (Fig. 4). Hence, in the most stable adsorption geometry on Rh(211) the contact between the molecule and the surface is significantly reduced, limiting the interaction between the molecule and the surface.

Summarizing the adsorption of phenol on Pt and Rh surfaces, the interaction is strongest on the terraces, while the molecule is repelled by the steps due to the inertness of the hydroxyl group to interact with the two substrates. Hence, the molecule will in first hand occupy terraces, which therefore will be most important when considering the catalytic activity of the molecule on the two substrates.

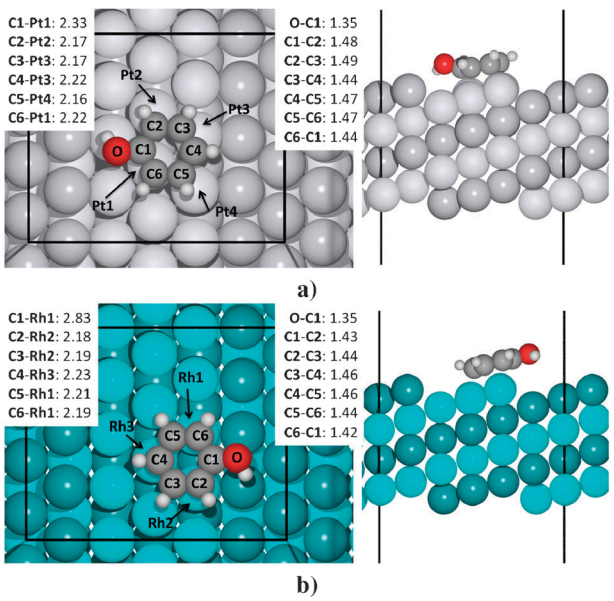

Fig. 4 Top and side views of the most stable configurations of phenol on (a) Pt(211) and (b) Rh(211). Atoms in alternating rows of the substrates are illustrated in different textures to visualize the steps between (111) terraces. The black lines indicate the unit cells used in the calculations. The tabulated bond lengths are in units of Å. Additional adsorption configurations can be found in the ESI.†

Table 1 Binding energies for the most stable adsorption configurations of phenol on Pt and Rh surfaces

Surface	Binding energy/eV
Pt(111)	2.23
Rh(111)	2.79
Stepped Pt(211)	1.59
Stepped Rh(211)	1.79

4.2 Dissociation of phenol into phenoxy

In order to determine the reaction energetics of the dehydrogenation of phenol into phenoxy we first studied the adsorption geometry of phenoxy on Pt(111) and Rh(111). Several parallel and vertical adsorption configurations were considered on both surfaces, with the most stable configurations illustrated in Fig. 5. It should be noticed that under vacuum phenoxy is a radical due to its unpaired electron centered on the oxygen atom. On Pt and Rh the radical intermediate is avoided due to electron exchange between the molecule and the surface, which can be visualized in the spin-polarized PDOS (see the ESI†). These systems are therefore well described in spin-paired calculations, which have been used throughout this section.

On both surfaces the molecule is adsorbed with the aromatic ring parallel to the surface, similar to the adsorption of phenol. However, on Pt(111) the oxygen atom is repelled by the surface even more than the hydroxyl group in the case of phenol adsorption. This repulsion is manifested by not only the oxygen atom, but also its adjoining carbon atom which is lifted away from the surface. Interestingly, on Rh(111) the entire molecule, including the oxygen atom, is in close contact with the surface. Hence, phenoxy interacts stronger with Rh(111) than with Pt(111).

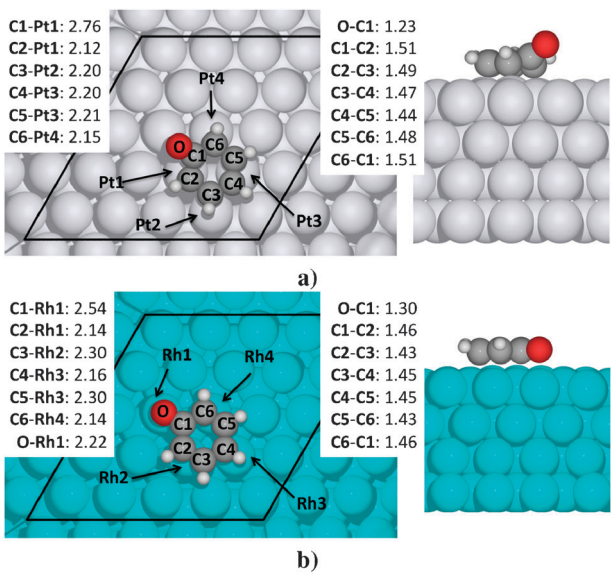

Fig. 5 Top and side views of the most stable configurations of phenoxy on (a) Pt(111) and (b) Rh(111). The black lines in the top views indicate the unit cells used in the calculations. The tabulated bond lengths are in units of Å. Additional adsorption configurations can be found in the ESI.†

The reaction energy E_{react} was defined as

$$E_{react} = E_{phenoxy+H} - E_{phenol}, \quad (2)$$

where $E_{phenoxy+H}$ is the total energy of phenoxy and atomic hydrogen adsorbed on Pt(111)/Rh(111) and E_{phenol} is the total energy of phenol adsorbed on Pt(111)/Rh(111). This definition of the reaction energy assumes that the dehydrogenated atoms adsorb on the surfaces as atomic hydrogen. The resulting reaction energy of the dehydrogenation of phenol into phenoxy is 0.26 eV on Pt(111) and −0.27 eV on Rh(111). In other words, on Pt(111) the reaction is endothermic, while on Rh(111) it is exothermic.

Transition state calculations were carried out to obtain further insight into the catalytic role of Pt(111) and Rh(111) in the dissociation of phenol into phenoxy. We used a combined NEB and dimer method approach to identify transition states, as outlined in Section 3 and which previously has been successful in describing even more complicated dehydrogenation processes.[19]

The resulting reaction pathways are illustrated in Fig. 6. For both surfaces, the dissociated H-atom is adsorbed on a hollow site close to the molecule in the final state **FIN**. Therefore, the final energy in each reaction is slightly different from the reaction energies reported above, which were obtained with a final state where the H-atom is adsorbed isolated on the surface. Both reaction paths have two energy barriers. Note that the second barrier, with transition state **TS2**, merely represents the surface diffusion of the H-atom into **FIN**; from a top to hollow site on Pt(111), while between adjacent hollow sites on Rh(111). It is nevertheless only the first barrier, with transition state **TS1**, which is associated with splitting-off the hydrogen. Hence, this state is the most relevant step in the dissociation of phenyl into phenoxy, and also the rate-limiting one in the two-step processes shown in Fig. 6. Therefore, in the following we will focus on the dehydrogenation step (**INI** → **INT**) for the two surfaces.

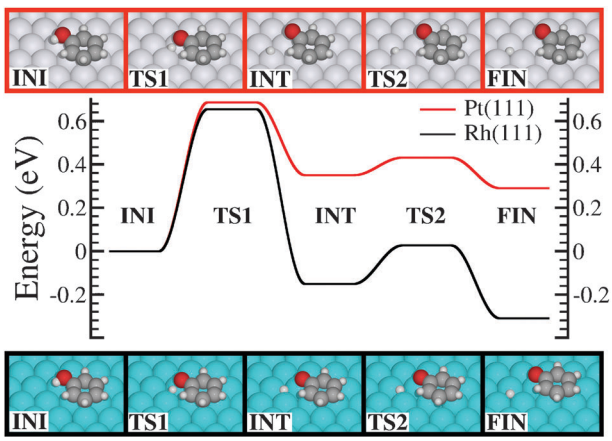

Fig. 6 Energy diagram illustrating the reaction barrier for the dissociation of phenol into phenoxy and atomic hydrogen on Pt(111) and Rh(111), depicted in the top and bottom of the figure, respectively. The dissociated H-atom was assumed to adsorb in equivalent hollow sites in the final state (**FIN**) for both surfaces. On Pt(111), the H-atom was found to be adsorbed on-top of a surface-atom in the intermediate state (**INT**), while for Rh(111) it is adsorbed in a hollow site adjacent to the molecule. **TS1** and **TS2** represent transition states (saddle points) along the reaction paths.

The reaction barriers to split off hydrogen from phenol are 0.69 eV and 0.66 eV on Pt(111) and Rh(111), respectively. This means that although the reaction is preferred on Rh(111) following the reaction energies, the reaction barriers are almost identical on the two surfaces. In other words, the reaction is expected to proceed at similar temperatures on Pt as on Rh. These results demonstrate the importance of considering reaction barriers when making conclusions about reaction kinetics.

It should be noted that the reaction is reversible, and for a finite coverage of molecules there is a probability for recombination of hydrogen and phenoxy into phenol. This is of particular importance for Pt, where the energy barrier of the reverse reaction is smaller than the barrier associated with the dissociation of phenol. In other words, our results suggest that for a finite coverage the dissociation will be observed at lower temperatures on Rh than on Pt, although the probability for the dissociation is similar on the two surfaces.

Ihm and White[10] observed with HREELS measurements that phenol dissociates into phenoxy below 200 K on Pt(111). On the other hand, Xu and Friend[11] observed with XPS that at 300 K there is only phenoxy on Rh(111). However, due to the absence of experimental data points between 100 K and 300 K on Rh(111), a more accurate comparison with experiment is not possible. Our results predict that a more detailed experimental study of phenol on Rh(111) would find that the dissociation occurs at even lower temperatures than on Pt(111).

ZrO_2 supported Pt and Rh catalysts have been tested in the HDO using guaiacol as a model component.[4] In this component both hydroxyl and methoxy groups are attached to the aromatic ring (Fig. 1). At 300 °C Rh shows better selectivity for deoxygenated products than Pt (oxygen to carbon ratio of 0.3 for guaiacol decreases to 0.15 on Pt and 0.05 on Rh).[4] Based on our results, the oxygen remains flat on the surface when phenoxy is adsorbed on Rh(111) but not on Pt(111). This may enable various reactions that affect the oxygen–carbon bond, explaining the higher deoxygenation activity of Rh compared to that of Pt.

5 Conclusions

The adsorption of phenol and its dissociation into phenoxy have been studied on Pt and Rh surfaces using DFT calculations. The results show that phenol adsorbs with the aromatic ring parallel to all the studied surfaces: Pt(111), Rh(111), stepped Pt(211) and stepped Rh(211). The adsorption is more preferred on the flat (111)-surfaces compared to the stepped (211)-surfaces. This results from the inertness of the hydroxyl group to interact with any of the surfaces. In addition, phenol adsorbs more preferably on Rh(111) than on Pt(111).

The dissociation of phenol into phenoxy is exothermic on Rh(111) while it is endothermic on Pt(111). However, the reaction barriers do not differ significantly between the surfaces, and the dissociation of phenol is expected at around the same temperatures for both surfaces in the low coverage limit. However, for finite coverages, the dissociation is predicted to proceed at lower temperatures on Rh(111) than on Pt(111). Our results are in qualitative agreement with the

available experimental observations.[10,11] However, a quantitative comparison between theory and experiments requires a more detailed experimental study of the dissociation of phenol.

In contrast to all the other systems we have studied, the oxygen atom in the phenoxy molecule is attracted by the Rh(111) surface. This may provide a higher deoxygenation activity of Rh compared to that of Pt. A challenge for future theoretical studies is the investigation of the deoxygenation of phenoxy on these surfaces. Finally, from a more general perspective, including temperature and pressure dependency into the theoretical models will be of great interest—and in particular—how the reaction proceeds under HDO conditions.

Acknowledgements

Dr Maija Honkela received funding from the Academy of Finland through Postdoctoral Researcher's Project No 115221. Prof. Mats Persson was funded by the Swedish Research Council (VR). Dr Felix Hanke and Adolfo Fuentes are thanked for useful comments and discussions. Computational resources at the University of Liverpool and IT Center for Science (CSC, Finland) are acknowledged.

References

1 R. Maggi and B. Delmon, *Biomass Bioenergy*, 1994, **7**, 245–249.
2 E. Furimsky, *Appl. Catal., A*, 2000, **199**, 147–190.
3 A. Bridgwater and M.-L. Cottam, *Energy Fuels*, 1992, **6**, 113–120.
4 A. Gutierrez, R. Kaila, M. Honkela, R. Slioor and A. Krause, *Catal. Today*, 2009, **147**, 239–246.
5 S. J. Jenkins, *Proc. R. Soc. London, Ser. A*, 2009, **465**, 2949–2976.
6 H. Orita and N. Itoh, *Appl. Catal., A*, 2004, **258**, 17–23.
7 N. Bonalumi, A. Vargas, D. Ferri and A. Baiker, *J. Phys. Chem. B*, 2006, **110**, 9956–9965.
8 Y. P. Tan, S. Khatua, S. J. Jenkins, J.-Q. Yu, J. B. Spencer and D. A. King, *Surf. Sci.*, 2005, **589**, 173–183.
9 R. Maggi and B. Delmon, *Stud. Surf. Sci. Catal.*, 1997, **106**, 99–113.
10 H. Ihm and J. M. White, *J. Phys. Chem. B*, 2000, **104**, 6202–6211.
11 X. Xu and C. Friend, *J. Phys. Chem.*, 1989, **93**, 8072–8080.
12 G. A. Somorjai and J. Carrazza, *Ind. Eng. Chem. Fundam.*, 1986, **25**, 63–69.
13 G. Kresse and J. Furthmüller, *Phys. Rev. B: Condens. Matter*, 1996, **54**, 11169–11186.
14 S. Bahn and K. Jacobsen, *Comput. Sci. Eng.*, 2002, **4**, 56–66.
15 P. E. Blöchl, *Phys. Rev. B: Condens. Matter*, 1994, **50**, 17953–17979.
16 G. Kresse and D. Joubert, *Phys. Rev. B: Condens. Matter Mater. Phys.*, 1999, **59**, 1758–1775.
17 J. P. Perdew, J. A. Chevary, S. H. Vosko, K. A. Jackson, M. R. Pederson, D. J. Singh and C. Fiolhais, *Phys. Rev. B: Condens. Matter*, 1992, **46**, 6671–6687.
18 M. Methfessel and A. T. Paxton, *Phys. Rev. B: Condens. Matter*, 1989, **40**, 3616–3621.
19 J. Björk, S. Stafström and F. Hanke, *J. Am. Chem. Soc.*, 2011, **133**, 14884–14887.
20 G. Henkelman, B. Uberuaga and H. Jónsson, *J. Chem. Phys.*, 2000, **113**, 9901–9904.
21 G. Henkelman and H. Jónsson, *J. Chem. Phys.*, 2000, **113**, 9978–9985.
22 G. Henkelman and H. Jónsson, *J. Chem. Phys.*, 1999, **111**, 7010–7022.
23 J. Kästner and P. Sherwood, *J. Chem. Phys.*, 2008, **128**, 014106–014111.
24 F. Abild-Pedersen, J. Greeley, F. Studt, J. Rossmeisl, T. R. Munter, P. G. Moses, E. Skúlason, T. Bligaard and J. K. Nørskov, *Phys. Rev. Lett.*, 2007, **99**, 016105.

